J Cereb Blood Flow Metab. Author manuscript; available in PMC 2009 June 26.

Published in final edited form as:
J Cereb Blood Flow Metab. 2009 February ; 29(2): 254–263. doi:10.1038/jcbfm.2008.106.

Protective effect of post-ischaemic viral delivery of heat shock proteins *in vivo*

Romina A Badin[1,2], **Michael Modo**[3,4], **Mike Cheetham**[5], **David L Thomas**[6], **David G Gadian**[1], **David S Latchman**[2], and **Mark F Lythgoe**[1]

[1]RCS Unit of Biophysics, UCL Institute of Child Health, London, UK

[2]Medical Molecular Biology Unit, UCL Institute of Child Health, London, UK

[3]MRC Centre for Neurodegenerative Research, Institute of Psychiatry, King's College London, London, UK

[4]Centre for the Cellular Basis of Behaviour, Institute of Psychiatry, King's College London, London, UK

[5]Division of Molecular and Cellular Neuroscience, Institute of Ophthalmology, University College London, London, UK

[6]Wellcome Trust High Field MR Research Laboratory, Department of Medical Physics, University College London, London, UK

Abstract

Heat shock proteins (HSPs) function as molecular chaperones involved in protein folding, transport and degradation and, in addition, they can promote cell survival both *in vitro* and *in vivo* after a range of stresses. Although some *in vivo* studies have suggested that HSP27 and HSP70 can be neuroprotective, current evidence is limited, particularly when HSPs have been delivered after an insult. The effect of overexpressing HSPs after transient occlusion of the middle cerebral artery in rats was investigated by delivering an attenuated herpes simplex viral vector (HSV-1) engineered to express HSP27 or HSP70 30 mins after tissue reperfusion. Magnetic resonance imaging scans were used to determine lesion size and cerebral blood flow at six different time points up to 1 month after stroke. Animals underwent two sensorimotor tests at the same time points to assess the relationship between lesion size and function. Results indicate that post-ischaemic viral delivery of HSP27, but not of HSP70, caused a statistically significant reduction in lesion size and induced a significant behavioural improvement compared with controls. This is the first evidence of effective post-ischaemic gene therapy with a viral vector expressing HSP27 in an experimental model of stroke.

Keywords

gene therapy; heat shock proteins; ischaemia; magnetic resonance imaging; neuroprotection

Correspondence: Dr RA Badin, Service de Neurovirologie, Commissariat à l'Energie Atomique FAR, Bat 02 P406, 18 Rue du Panorama, 92265 Fontenay-aux-Roses, France. E-mail: rabadin@yahoo.com.

Europe PMC Funders Author Manuscripts

Introduction

Stroke is a major cause of death and disability in the Western world. Approximately 25% of all strokes lead to death, yet 80% of survivors experience motor weakness and 30% have long-term disability (Bogousslavsky *et al*, 1988). Ischaemic stroke accounts for approximately 85% of all clinical cases and the patient's outcome strongly depends on the duration of the stroke. Although many clinical trials have been attempted, their success has been poor (de Keyser *et al*, 1999; Fisher and Schaebitz, 2000) and thrombolytic therapy applied within a very narrow therapeutic window (~3 h) has been the only available pharmaceutical treatment for stroke patients for over 10 years.

Several neuroprotection studies have identified heat shock proteins (HSPs) 27 and 70 as potential therapeutic agents. These cellular chaperones assist in the folding of nascent polypeptides or proteins that have been denatured because of environmental stress. Their upregulation is an endogenous response to stress that is highly conserved across eukaryotes and prokaryotes (Latchman, 2004). Accelerating cell repair after stress is related not only to their chaperoning activities but also to their ability to present denatured proteins to the protea-some for degradation and to their anti-apoptotic functions (Kiang and Tsokos, 1998; Hershko and Ciechanover, 1998; Sharp *et al*, 1999; Latchman, 2004). In view of the pre-ischaemic evidence of protection previously described for HSP27 (Aron Badin *et al*, 2006), we now report on the effect of post-ischaemic viral delivery of HSPs on lesion size in a transient model of stroke in rats. One study to date has histologically determined that post-ischaemic viral overexpression of HSP70 caused no reduction in lesion size, but no assessment of behavioural improvement was performed (Hoehn *et al*, 2001).

One of the limitations of animal neuroprotective experiments is that long-term functional recovery in motor tasks is not always assessed. The bilateral asymmetry and foot-fault tests have often been used to assess long-lasting sensorimotor neglect of the contralateral limbs resulting from unilateral brain damage (Schallert *et al*, 1982; Modo *et al*, 2000). The bilateral asymmetry test mimics the contralateral neglect syndrome caused by damage to the parietal cortex and the tactile extinction observed in patients with unilateral stroke (Rose *et al*, 1994). The foot-fault test measures spontaneous locomotor activity, motor coordination, and sensorimotor integration (Hunter *et al*, 1998) and has been shown to provide a good indication of motor impairment because of unilateral middle cerebral artery (MCA) occlusion up to 3 weeks after stroke (Markgraf *et al*, 1992; Aronowski *et al*, 1996).

In this study, an attenuated herpes simplex viral (HSV) vector was intracerebrally microinjected to deliver HSP27, HSP70, or control LacZ protein 30 mins after reperfusion. Non-invasive magnetic resonance imaging (MRI) techniques were used to measure lesion size, water diffusion, and cerebral blood flow (CBF) at six different time points, from 24 h to 1 month after induction of ischaemia. Moreover, behavioural tests were concomitantly run to assess whether gene therapy could improve the functional deficits caused by the stroke in treated animals compared with controls. Finally, colocalization of HSP27 and synaptophysin was assessed to investigate the role of this chaperone in one of the possible mechanisms of brain reorganization after stroke.

Materials and methods

All animal care and procedures were performed in accordance with the UK Animals (Scientific Procedures) 1986 Act.

Intracerebral Microinjections and Middle Cerebral Artery Occlusion

Three groups ($n = 6$) of adult male Sprague–Dawley rats (220–280 g) were anaesthetized with 2% isoflurane in 70:30 N_2O to O_2 and placed in a stereotaxic frame (Kopf, Germany). A midline incision was made on the head, the skin was retracted and a burr hole was made on the skull over the right striatum (bregma coordinates: AP, + 0.10 cm; L, −0.35 cm; V, −0.50 cm). Under the microscope, a 290 μm Monocryl suture (Ethicon, UK) with an araldite-coated tip was introduced into the right common carotid artery up to the origin of the MCA for 30 mins and retracted. Stereotaxic intracerebral microinjections with an attenuated HSV type 1 vector engineered to express HSP27, HSP70, or LacZ were performed into the right striatum 30 mins after reperfusion, as previously described (Aron Badin *et al*, 2006). A microsyringe pump (WPI, UK) was used to deliver 2.5 μl of HSV-LacZ, HSVHSP70, and HSV-HSP27 (at 1×10^6 PFU/μl) to the right striatum at a constant rate of 0.25 μl/min. Throughout the surgery, rectal temperature was maintained at 37±1°C by a heating blanket. The whole procedure took 2 h and the animals were left to recover for 24 h before scanning, with free access to food and water.

Magnetic Resonance Imaging

Scans were performed on a 2.35 T horizontal bore magnet (Oxford Instruments, UK) interfaced to an SMIS console (Guildford, UK). All animals ($n = 18$) were anaesthetized with 2% halothane in a 70:30 N_2O to O_2 mix delivered through nose cone and placed on a probe with bite and ear bars securing the head to minimize movement artefacts. Physiologic parameters monitored included electrocardiography recordings and rectal temperature, which was maintained at 37±1°C using an air warming system.

The imaging protocol included a multislice T_2-weighted spin echo sequence for the determination of lesion size and three single-slice echo planar imaging sequences: T_1 and continuous arterial spin labelling for the determination of CBF, and a single-shot isotropic diffusion-weighted imaging sequence (Wong *et al*, 1995) to determine the apparent diffusion coefficient (ADC). All echo planar imaging sequences were run on a single 2-mm-thick coronal slice located in the centre of the MCA territory (0.5 mm from bregma). The matrix size was 128×64 and the field of view was 40×20 mm. The sequence parameters were diffusion-weighted imaging (TR = 1,500 ms, TE/2 = 58 ms, b values = 6 and 1,187 s/mm^2, 64 averages); T_1 (TR = 2,000 ms, TE/2 = 18 ms, TI array = 284, 434, 634, 834, 1,234, 1,734, 2,734, and 3,734 ms, 16 averages); and continuous arterial spin labelling (interexperimental delay = 1,000 ms, TE/2 = 18 ms, 44 averages). The inversion slice was positioned approximately 13 mm from the back of the cerebellum and labelling and reference scans were obtained with a 500 ms delay time (Alsop and Detre, 1996). The multislice T_2-weighted SE sequence (TR = 1,500 ms, TE = 120 ms, 8 averages, 9 slices) was run on 1-mm-thick slices to determine the lesion volume. The centre slice of the multislice data set was determined by anatomic landmarks on visual inspection of pilot coronal scans and not by the maximal lesion area. Total scan time was 35 mins.

Image Processing and Data Analysis

Quantitative maps were obtained by reconstructing all images with IDL Software version 5.2 (Research Systems Inc., Colorado, USA). T_1 maps and continuous arterial spin labelling subtraction images (control—labelled) were used to calculate CBF maps (Thomas *et al*, 2000). All the lesion area/volume measurements and regions of interest were segmented manually on all processed images using SMIS Image Display version 3.7. The resulting lesion areas per slice were used to determine lesion volume across the whole brain. Moreover, a regional analysis was performed on the T_2-weighted multislice data set based on knowledge of the vascular territories in the rat brain (Paxinos, 1995). Slices were grouped into three regions: the frontal region (slices 1 and 2), the mid MCA territory region

(slices 3, 4, 5, and 6), and the posterior region (slices 7, 8, and 9). A restricted maximum likelihood analysis of the longitudinal lesion volume data was performed using a full random coefficients model, assuming a linear dependence on time. The probability values were obtained using the F-test and considered significant at $P < 0.05$. These calculations were performed using SAS PROC MIXED (SAS Institute, 1999). The CBF and behavioural test results were analysed using repeated-measures analysis of variance (SPSS 12.0.1; SPSS Inc., USA) with groups as the between-subjects factor and assessment time points as the within-subjects factor. Adjusted degrees of freedom are quoted for all calculations. Standard *t*-tests were used for regression analysis and end-point comparisons. All data are presented as mean±standard error (s.e.m.).

Behavioural Tests

Bilateral asymmetry and foot-fault tests were performed on all animals as previously described (Schallert *et al*, 1982; Hernandez and Schallert, 1988; Modo *et al*, 2000). Two trials were performed per time point on all three groups of animals ($n = 6$), starting at 3 days and up to 1 month after stroke.

Bilateral asymmetry test—Time to removal of a strip of brown packing tape from each paw was measured. The order of the application (i.e., left or right paw first) was reversed for each consecutive trial, which lasted 180 secs. Tests were not considered or repeated if the animal was unable to remove the tape from both paws. If the tape was not removed from one paw, the test was assigned the maximum value of 180 secs for that paw.

Foot-fault test—Animals were placed at one end of a homebuilt elevated frame covered with a 7-cm hole mesh wire. The total number of steps and the correct or incorrect placement of the left affected forelimb (contralateral to the infarction) were recorded. Each trial lasted 60 secs and the test was discarded and not repeated if the animal took less than 10 steps.

Immunohistochemistry

Animals were terminally anaesthetized and decapitated. Brains were extracted, flash frozen in cooled isopentane (2-methyl-butane; BDH, UK), sliced into 10 μm cryosections (Bright Instruments, UK), and air dried before rehydration in phosphate-buffered saline and fixation in 3.7% parafolmadehyde for 15 mins. The sections were then incubated in blocking solution (3% bovine serum albumin and 10% donkey or goat serum in phosphate-buffered saline; Stratech Scientific Ltd, UK) for 1 h at room temperature. Sections were stained with rabbit polyclonal anti-HSP27 (1:200, product no. SPA-801; Stressgen Biotechnologies, UK) and mouse monoclonal synaptophysin (1:500, product no. S5768; Sigma-Aldrich, UK) primary antibodies overnight at 4°C. Cy2 AffiniPure Donkey Anti-Mouse IgG (H + L; 1:500) (product no. 715-225-151; Stratech Scientific Ltd) and Cy3 AffiniPure Donkey Anti-Rabbit IgG (H + L; 1:500) (product no. 711-165-152; Stratech Scientific Ltd) fluorescent secondary antibodies were used. 4′,6-Diamidino-2-phenylindole dihydrochloride (Sigma-Aldrich) was added to the secondary antibodies (at 2 μg/ml) to counterstain the nuclei. Fluorescence was visualized with an LSM510 confocal microscope (Carl Zeiss, Hertfordshire, UK) and viewed with Zeiss LSM Image Browser version 3.5.0.376 software.

Results

Gene Therapy and Lesion Size

Three groups of six animals were microinjected with HSV-HSP27, HSV-HSP70, or HSV-LacZ as a control 30 mins after tissue reperfusion. Figure 1 shows the centre slice (slice 5) of multislice T_2-weighted spin echo image data sets obtained 24 h, 1 week, and 3 weeks

after transient MCA occlusion and the averaged total lesion volumes measured from the images at all time points.

A mixed-model regression analysis was performed to assess the evolution of the lesion over time. *t*-Tests on the individual regression slopes indicated a significant change in the mean lesion volume in HSP27-treated animals over time (−0.59±0.2 mm^3 per day; $P = 0.01$). The regression slopes for the two other groups were −0.08±0.2 mm^3 per day for HSP70 and −0.07±0.2 mm^3 per day for LacZ-injected animals respectively and did not achieve statistical significance ($P_{HSP70} = 0.72$; $P_{LacZ} = 0.75$). The mean absolute lesion volume estimates at 28 days were 48.5±8.3 mm^3 for HSP27-injected rats, 68.9±8.3 mm^3 for HSP70-injected rats, and 71.5±8.3 mm^3 for LacZ-injected animals. The difference in mean lesion volume between HSP27-treated and LacZ-injected controls was statistically significant (difference = 23±11.8 mm^3; $P = 0.05$), whereas no significant difference was found between HSP70-treated animals and controls (difference = 2.6±11.8 mm^3; $P = 0.8$).

A regional analysis was performed on the multislice data by grouping frontal slices (region 1 (R_1)= slices 1, and 2), mid MCA territory slices (R_2 = slices 3, 4, 5, and 6), and posterior slices (R_3 = slices 7, 8, and 9) (Figure 2). Regression analysis indicated that the three groups differed in their regional dependence ($P = 0.02$). The regional population mean volume estimates at 28 days suggested that HSP27 treatment was more effective in the posterior region than in the frontal and mid regions (HSP27 R_1 = 0.68±3.1 mm^3, R_2 = 33.8±3.1 mm^3, R_3 = 15.4± 3.1 mm^3; HSP70 R_1 = 3.7±3.1 mm^3, R_2 = 36.5±3.1 mm^3, R_3 = 28.7±3.1 mm^3; LacZ R_1 = 1.1±3.1 mm^3, R_2 = 38.9±3.1 mm^3; R_3 = 31.6±3.1 mm^3). In fact, the differences (Δ) in mean absolute lesion volumes in regions 1 and 2 between HSP27-treated rats and controls were 1.8±4.4 ($P = 0.4$) and 5.05±4.4 mm^3 ($P = 0.2$), whereas region 3 presented a significant 16.1±4.4 mm^3 difference in lesion volume ($P = 0.0003$). No differences were found when comparing mean absolute lesion volume estimates over time in regions 1, 2, and 3 in HSP70-treated rats and controls (Δ_{R1} =2.6±4.4 mm^3, $P = 0.6$; Δ_{R2} = 2.3±4.4 mm^3, $P = 0.6$; Δ_{R3} = 2.9±4.4 mm^3, $P = 0.5$).

A comparison between diffusion-weighted and T_2-weighted single-slice images obtained at 24 h after stroke induction and viral microinjection showed that the area of low ADC of water was larger than the lesion on T_2 maps in HSP27-treated animals only. The mean difference in affected areas between the two images was calculated as the percentage of pixel numbers over the total pixels in the ipsilateral hemisphere and was 19.1%±1.5% for HSP27-treated animals, 3.1%±0.6% for HSP70-treated animals, and 2.1%±0.5% for LacZ controls (HSP27 versus LacZ: $P = 0.00004$; HSP70 versus LacZ: $P = 0.2$). Figure 3 shows this difference for all animals in all three groups.

Cerebral blood flow was measured at 24 h, 72 h, 1 week, 2 weeks, 3 weeks, and 4 weeks after occlusion reperfusion. Values in the ischaemic hemisphere for treated and control animals are presented in Table 1, expressed as a percentage of flow in the contralateral hemisphere. All CBF values were above the ischaemic threshold (Kohno *et al*, 1995) and statistical analysis in fact showed no significant differences between the groups (controls versus HSV-HSP27 ($F(2,15) = 1.9$, $P > 0.2$); controls versus HSV-HSP70 ($P > 0.9$) at all time points after reperfusion.

Gene Therapy and Functional Recovery

Bilateral asymmetry test—The sensorimotor asymmetry test showed that all animals subjected to transient MCA occlusion preferentially removed the tape from the forelimb ipsilateral to the ischaemic hemisphere first. The time to removal of the tape from left (affected) and right (unaffected) paws was recorded at five different time points: 72 h, 1 week, 2 weeks, 3 weeks, and 4 weeks. There was a marked difference in removal time

between the left and right paws for all three groups and such sensory neglect persisted throughout the period tested. Repeated-measures analysis of variance showed significant main effects for group and for time (group: $F(2,13) = 5.5$, $P = 0.02$; time: $F(2.6,34.4) = 3.9$, $P = 0.02$), but no significant interaction (group×time: $F(5.3,34.4) = 0.4$, $P = 0.8$). However, a t-test comparison at the first time point tested indicated that there was no significant difference between the groups at 72 h after stroke (LacZ versus HSP27, $P = 0.34$; LacZ versus HSP70, $P = 0.37$), whereas a difference was seen in HSP27-treated animals compared with controls at 4 weeks (LacZ versus HSP27, $P = 0.05$; LacZ versus HSP70, $P = 0.44$; Figure 4).

Foot-fault test—At 72 h after occlusion animals were placed in an elevated mesh wire grid for 1 min and the total number of paired steps were counted together with the number of foot faults or errors in which the animal misplaced the left forelimb such that it fell through the grid. The total number of errors for the affected forelimb was recorded. The total number of steps and the percentage of correct steps for all animals at all time points tested are presented in Table 2. The total number of left steps was not significantly different between either HSP27-treated and controls ($P = 0.2$) or HSP70-treated animals and controls ($P = 0.2$). Similarly, there were no significant differences in the total number of right steps between the groups at all time points tested (LacZ versus HSP27, $P = 0.2$; LacZ versus HSP70, $P = 0.07$). All animals showed some degree of impairment in this task on the first few weeks after MCA occlusion but a significant group effect was found when comparing the percentage of correct steps in all three groups (group×time: $F(5.7,42.4) = 0.712$, $P = 0.634$; group: $F(2,15) = 29.88$, $P = 0.0001$). In fact, a significant difference in the percentage of correct steps was found when comparing HSP27-treated animals to controls (group×time: $F(2.6,25.8) = 149.03$, $P = 0.68$; group: $F(1,10) = 19.5$, $P = 0.001$). HSP70-treated animals, however, appeared to perform worse than controls in this task but this difference in behaviour observed between the groups only reached a borderline statistical significance (group×time: $F(2.3,23.4) = 0.48$, $P = 0.66$; group: $F(1,10) = 4.98$, $P = 0.05$).

Histology

In view of the behavioural improvement observed in HSP27-treated animals, fluorescent immunohistochemistry experiments were conducted to assess whether this chaperone had an involvement in plasticity. Rat brains were extracted at 4 weeks after stroke induction and cryostat sections were stained for HSP27 and synaptophysin, a marker protein for synaptogenesis. Figure 5 shows that both proteins are highly expressed in the basal ganglia and the border of the scar but no colocalization was observed.

Discussion

The aim of the study was to investigate neuroprotection *in vivo* after post-ischaemic delivery of an HSV-based vector expressing HSP27 or HSP70 in a rat focal model of transient cerebral ischaemia. Longitudinal MRI measurements enabled the assessment of the effect of HSP27 and HSP70 treatment on lesion size at 1, 3, 7, 14, 21, and 28 days after stroke. Behavioural tests were performed at the same imaging time points to provide an indication of sensorimotor impairment and recovery over time. Immunohistochemistry experiments were performed at 4 weeks to investigate whether HSP27 colocalized with synaptophysin and was therefore involved in plasticity and brain reorganization after stroke. The model of stroke chosen for this *in vivo* study has been previously reported to produce a reproducible lesion encompassing the right cortex and basal ganglia (Aron Badin *et al*, 2006). In addition, direct intrastriatal microinjection of viral vectors was previously observed to yield high levels of protein expression in the ipsilateral hemisphere of HSP-treated and LacZ-injected control animals (Aron Badin *et al*, 2006). The multislice T_2-weighted scans, indicative of

vasogenic oedema, were used to determine lesion size. These images showed a marked reduction in lesion volume in HSV-HSP27-treated animals compared with HSV-LacZ controls. In contrast, HSV-HSP70 treatment had no effect on lesion size. Moreover, regional analysis of lesion volume suggested that HSP27 treatment was most effective on posterior slices compared with controls. Interestingly, direct comparison of the lesion defined on ADC and T_2-weighted maps at 24 h indicated that the area of abnormal ADC was almost 20% larger than the area of vasogenic oedema in HSP27-treated animals, whereas no differences were found in HSP70- or LacZ-injected animals. All CBF values obtained 24 h and up to 4 weeks after occlusion reperfusion were above the ischaemic threshold and similar in the three groups. Behavioural studies indicate that the sensorimotor skills of HSV-HSP27-injected animals were less impaired immediately after stroke and showed improvement over time. Fluorescent immunohistochemistry indicated that HSP27 did not colocalize with synaptophysin, suggesting it is not directly contributing to behavioural improvement in HSP27-treated animals by enhancing synaptogenesis. However, the fact that this chaperone was still expressed in the brain at 4 weeks after ischaemia induction in HSP27-treated animals also suggests it could be involved in functional recovery through a different mechanism.

MRI Findings: Lesion Size

The changes in lesion volume over time were different among the three groups. Multislice T_2-weighted images acquired at 24, 72 h, and weekly for 1 month after transient occlusion of the MCA indicate that overall lesion volume at 4 weeks was 25% smaller in HSP27-treated animals whereas LacZ-injected controls showed no reduction over time. HSP70 treatment caused no reduction in lesion size at 4 weeks and the lesion volumes were not significantly different from those obtained for LacZ controls at the same time point. Such difference in the progression of the lesion over time could be due to the fact that unlike other pharmacotherapies, the viral vector used in this study is continuously expressing HSP27 and enhancing an endogenous upregulation of this protein that has been extensively reported. This gives rise to a large therapeutic window that could have not only acute but also additive effects over time.

Interestingly, MRI measurements at 24 h suggest that HSP27-treated animals have a region of severely compromised tissue (T_2-weighted lesion) with a surrounding area of compromised tissue (diffusion change), which is not apparent in the controls. The fact that in this study only HSP27-injected animals show an area of low ADC outside the region of T_2-weighted change (which was smaller than in the control and HSP70 groups) suggests that the post-ischaemic treatment with HSP27 may be able to prevent compromised tissue from going onto infarction most likely by reducing mitochondrial dysfunction and consequent energy failure and interfering with the apoptotic cascade. However, we cannot rule out the possibility that there may be some residual neuronal loss or gliosis in the brain regions that showed resolution of the T_2 changes (Wegener *et al*, 2006).

Regional analysis suggests that although the central slices show an effect consistent with the mismatch between the diffusion and T_2 data, posterior slices are more protected against stroke progression in HSP27-treated animals only. These posterior regions could correspond to a penumbral zone that proceeds to infarction over time without intervention as seen in HSV-LacZ-injected MCA-occluded controls (Figure 2).

Lesion Size and Behaviour

Several studies have found strong correlations between infarct size and neurobehaviour (Minematsu and Fisher, 1993; Belayev *et al*, 1995; Rogers *et al*, 1997). In agreement with this literature, improvements on sensorimotor tasks were seen HSP27-treated animals, which

also showed a reduction in lesion size compared with controls. Conversely, there was no evidence of functional improvement or reduction in lesion size in the HSP70-treated animals. In fact, the bilateral asymmetry test results show that the initial sensory deficit was not significantly different in any of the groups, suggesting that the sparing of tissue in HSP27-treated animals is accompanied by a functional recovery over time (Figure 4). Similarly, the foot-fault test indicated that HSP27-treated animals present a higher number of correct steps than controls at all time points assessed, whereas HSP70-treated animals seem to perform worse than controls (Table 2).

It is interesting to note that differences in lesion size in the posterior regions and differences in behavioural improvement became more apparent at 2 weeks after MCA occlusion in HSP27-treated animals compared with controls. Other animal studies using MRI to investigate functional activation after stroke in combination with behavioural tests have shown correlations between contralateral limb impairment and activation impairment in the lesioned cortex (Dijkhuizen *et al*, 2001). The contralateral hemisphere appears to initially compensate for the sensorimotor deficit caused by the stroke but at 14 days the activation balance is restored once the ipsilateral hemisphere recovers and reorganizes. Furthermore, a different study by the same group later established that the degree of injury determines the extent of activation shift to the contralateral hemisphere at early time points and that the extent of functional recovery over time is related to the preservation or restoration of activation in the lesioned hemisphere (Dijkhuizen *et al*, 2003). In this context, the reduction in lesion size found in HSP27-treated animals in the present study could be associated with an increased preservation of function in the ipsilateral hemisphere and may explain why these animals exhibit behavioural improvements compared with untreated controls.

HSP27 and Neuroprotection

The mechanisms by which HSP27 could prevent cellular damage and therefore lesion size from expanding are uncertain. Both HSP27 and HSP70 are potentially involved in improving cell survival by refolding denatured proteins and/or interfering with apoptotic pathways (Mehlen *et al*, 1996; Saleh *et al*, 2000; Mosser *et al*, 2000; Paul *et al*, 2002; Benn *et al*, 2002; Akbar *et al*, 2003; Latchman, 2004). However, there is currently not enough evidence to distinguish specific functions that might make one chaperone more suitable than the other.

One of the most salient advantages that HSP27 might have over HSP70 in an ischaemic environment is its ATP independence (Rogalla *et al*, 1999; Garrido, 2002; Riordan *et al*, 2005). Moreover, this chaperone has been implicated in antioxidant mechanisms by causing a decrease in intracellular reactive oxygen species and thus protecting against cell death because of oxidative stress (Mehlen *et al*, 1996; Samali and Orrenius, 1998). Cytoskeletal stabilization by capping and decapping of actin filaments could protect such microfilaments from degradation and depolymerization because of stress (Guay *et al*, 1997). *In vitro* experiments in astroglia have shown that HSP27 interacts with glial fibrillary acidic protein and vimentin and prevents stress-induced aggregation of these proteins, thus promoting cell stabilization and survival (Perng *et al*, 1999). Other experiments investigating the role of endogenous HSP27 highlight its involvement in plasticity. Astroglial expression of HSP27 has been observed in the immature and mature rat brain *in vivo* after different insults including ischaemia, excitotoxicity, axonal degeneration, and photo-thrombotic injury, suggesting that this is a common defence mechanism in the brain (reviewed in Acarin *et al*, 2002). Moreover, there is evidence supporting the role of HSP27 in protecting not only the cells where it is expressed (i.e., astroglia), but also the surrounding damaged tissue (Acarin *et al*, 2002). This and other studies looking at HSP27 in epilepsy rat models suggest that there is a relationship between HSP27 expression and areas undergoing anatomic reorganization and axonal sprouting (Kato *et al*, 1994, 1999). Our immunohistochemistry

experiments, however, were unable to establish colocalization between HSP27 and synaptophysin. This does not exclude the possibility that HSP27 is implicated in the structural and functional reorganization of the brain occurring after stroke through a different pathway. In fact, the significant behavioural improvement observed in HSP27-treated animals suggests, therefore, that this chaperone might be exerting its protective function through a mechanism other than synaptogenesis.

The post-ischaemic therapy results are in line with previous findings, where pre-ischaemic micro-injections of HSV-HSP27 and not HSV-HSP70 caused a significant 44% reduction in lesion size (Aron Badin *et al*, 2006). Contrary to the present experiments, the only other post-ischaemic study to date using an HSV viral vector to deliver HSP70 to the ischaemic brain after 0.5 and 2 h of MCA occlusion showed improved survival of striatal neurones but had no effect on lesion size (Hoehn *et al*, 2001). A significant reduction in lesion size in our post-ischaemic study was seen in HSP27-treated animals and not in HSP70-treated animals. This discrepancy could be because of a number of differences between the two studies, such as the animal model, the delivery method chosen, the HSP expression levels and the lesion size assessment and time. Hoehn *et al*. induced 60 mins of MCA occlusion followed by reperfusion (as opposed to 30 mins in this study), used an amplicon HSV vector and gave two injections in the ipsilateral and contralateral striatum respectively, assessed damage at 48 h only, and used a semiquantitative histologic scale to determine lesion size. Such differences in study design and methodology have been thought to underlie the variable results obtained for HSP70 transgenic mouse models of stroke as well as the rat studies using viral vectors to deliver HSP70 before and after stroke. Consistency between our pre- and post-ischaemic *in vivo* studies indicates that at least in this model HSP27 has an obvious neuroprotective effect and HSP70 does not.

In conclusion, efficient therapy for stroke is still lacking and the increasing number of therapies attempting repair and regeneration have enhanced the need for investigation of functional outcome in clinical and experimental stroke. The study presented here addresses both these issues by evaluating the effects of HSP treatment on stroke on the basis of longitudinal non-invasive MRI measurements of lesion size and long-term sensorimotor testing. Such novel combination of techniques has allowed us to show the neuroprotective post-ischaemic effect of HSP27 overexpression for the first time and further supports a correlation between reductions in functional impairment and in lesion size. The mechanisms underlying the protective effect of HSP27 *in vivo* have not been elucidated yet. A possible explanation is that the tissue that was salvaged by early therapeutic intervention with HSP27 undergoes some degree of functional preservation that is absent in controls.

Acknowledgments

We thank Dr Martin King for the statistical analysis and critical advice.

This work was supported by the Wellcome Trust and the Biotechnology and Biological Sciences Research Council and a UCL Institute of Child Health CHRAT Studentship.

References

Acarin L, Paris J, Gonzalez B, Castellano B. Glial expression of small heat shock proteins following an excitotoxic lesion in the immature rat brain. Glia. 2002; 38:1–14. [PubMed: 11921199]

Akbar MT, Lundberg AMC, Liu K, et al. The neuroprotective effects of heat shock protein 27 over-expression in transgenic animals against kainate-induced seizures and hippocampal cell death. J Biol Chem. 2003; 278:19956–65. [PubMed: 12639970]

Alsop DC, Detre JA. Reduced transit-time sensitivity in non-invasive magnetic resonance imaging of human cerebral blood flow. J Cereb Blood Flow Metab. 1996; 16:1236–49. [PubMed: 8898697]

Aron Badin R, Lythgoe MF, van der Weerd L, et al. Neuroprotective effects of virally delivered HSPs in experimental stroke. J Cereb Blood Flow Metab. 2006; 26:371–81. [PubMed: 16079790]

Aronowski J, Samways E, Strong R, Rhoades HM, Grotta JC. An alternative method for the quantitation of neurological damage after experimental middle cerebral artery occlusion in rats: analysis of behavioural deficit. J Cereb Blood Flow Metab. 1996; 16:705–13. [PubMed: 8964811]

Belayev L, Busto R, Zhao W, Ginsberg MD. HU-211, a novel non-competitive *N*-methyl-d-aspartate antagonist, improves neurological deficit and reduces infarct volume after reversible focal ischaemia in the rat. Stroke. 1995; 26:2313–20. [PubMed: 7491657]

Benn SC, Perrelet D, Kato AC, et al. Hsp27 upregulation and phosphorylation is required for injured sensory and motor neuron survival. Neuron. 2002; 36:45–56. [PubMed: 12367505]

Bogousslavsky J, Van Melle G, Regli F. The Lausanne Stroke Registry: analysis of 1000 consecutive patients with first stroke. Stroke. 1988; 19:1083–92. [PubMed: 3413804]

de Keyser J, Sulter G, Luiten PG. Clinical trials with neuroprotective drugs in acute ischaemic stroke: are we doing the right thing? Trends Neurosci. 1999; 22:535–40. [PubMed: 10542428]

Dijkhuizen RM, Ren J, Mandeville JB, et al. Functional magnetic resonance imaging of reorganization in rat brain after stroke. Proc Nat Acad Sci USA. 2001; 98:12766–71. [PubMed: 11606760]

Dijkhuizen RM, Singhal AB, Mandeville JB, et al. Correlation between brain reorganization, ischemic damage, and neurologic status after transient focal cerebral ischemia in rats: a functional magnetic resonance imaging study. J Neurosci. 2003; 23:510–7. [PubMed: 12533611]

Fisher M, Schaebitz W. An overview of acute stroke therapy: past, present, and future. Arch Intern Med. 2000; 160:3196–206. [PubMed: 11088079]

Garrido C. Size matters: of the small HSP27 and its large oligomers. Cell Death Differ. 2002; 9:483–5. [PubMed: 11973606]

Guay J, Lambert H, Gingras-Breton G, et al. Regulation of actin filament dynamics by p38 map kinase-mediated phosphorylation of heat shock protein 27. J Cell Sci. 1997; 110:357–68. [PubMed: 9057088]

Hernandez TD, Schallert T. Seizures and recovery from experimental brain damage. Exp Neurol. 1988; 102:318–24. [PubMed: 3197789]

Hershko A, Ciechanover A. The ubiquitin system. Annu Rev Biochem. 1998; 67:425–79. [PubMed: 9759494]

Hoehn B, Ringer TM, Xu L, et al. Overexpression of HSP72 after induction of experimental stroke protects neurons from ischemic damage. J Cereb Blood Flow Metab. 2001; 21:1303–9. [PubMed: 11702045]

Hunter AJ, Mackay KB, Rogers DC. To what extent have functional studies of ischaemia in animals been useful in the assessment of potential neuroprotective agents? Trends Pharmacol Sci. 1998; 19:59–66. [PubMed: 9550943]

Kato H, Liu Y, Kogure K, Kato K. Induction of 27-kDa heat shock protein following cerebral ischemia in a rat model of ischemic tolerance. Brain Res. 1994; 634:235–44. [PubMed: 8131073]

Kato K, Katoh-Semba R, Takeuchi IK, et al. Responses of heat shock proteins hsp27, alphaB-crystallin, and hsp70 in rat brain after kainic acid-induced seizure activity. J Neurochem. 1999; 73:229–36. [PubMed: 10386975]

Kiang JG, Tsokos GC. Heat shock protein 70 kDa: molecular biology, biochemistry and physiology. Pharmacol Ther. 1998; 80:183–201. [PubMed: 9839771]

Kohno K, Hoehn-Berlage M, Mies G, Back T, Hossmann KA. Relationship between diffusion-weighted MR images, cerebral blood flow, and energy state in experimental brain infarction. Magn Res Imaging. 1995; 13:73–80.

Latchman DS. Protective effects of heat shock proteins in the nervous system. Curr Neurovasc Res. 2004; 1:21–7. [PubMed: 16181063]

Markgraf CG, Green EJ, Hurwitz BE, Morikawa E, et al. Sensorimotor and cognitive consequences of middle cerebral artery occlusion in rats. Brain Res. 1992; 575:238–46. [PubMed: 1571783]

Mehlen P, Schulze-Osthoff K, Arrigo AP. Small stress proteins as novel regulators of apoptosis: heat shock protein 27 blocks Fas/APO-1- and staurosporine-induced cell death. J Biol Chem. 1996; 271:16510–4. [PubMed: 8663291]

Minematsu K, Fisher M. MK-801 reduces extensive infarction after suture middle cerebral artery occlusion in rats. Cerebrovasc Dis. 1993; 3:99–104.

Modo M, Stroemer RP, Tang E, Veizovic T, et al. Neurological sequelae and long-term behavioural assessment of rats with transient middle cerebral artery occlusion. J Neurosci Methods. 2000; 194:99–109. [PubMed: 11163416]

Mosser DD, Caron AW, Bourget L, et al. The chaperone function of hsp70 is required for protection against stress-induced apoptosis. Mol Cell Biol. 2000; 20:7146–59. [PubMed: 10982831]

Paul C, Manero F, Gonin S, et al. Hsp27 as a negative regulator of cytochrome c release. Mol Cell Biol. 2002; 22:816–34. [PubMed: 11784858]

Paxinos, G. The rat nervous system. 2nd edn.. London: Academic Press: 1995.

Perng MD, Muchowski PJ, van den IJssel P, et al. The cardiomyopathy and lens cataract mutation in alphaB-crystallin alters its protein structure, chaperone activity, and interaction with intermediate filaments *in vitro*. J Biol Chem. 1999; 274:33235–43. [PubMed: 10559197]

Riordan M, Sreedharan R, Wang S, Thulin G. HSP70 binding modulates detachment of Na-K-ATPase following energy deprivation in renal epithelial cells. Am J Physiol Renal Physiol. 2005; 288:F1236–42. [PubMed: 15701813]

Rogalla T, Ehrnsperger M, Preville X, Kotlyarov A, et al. Regulation of Hsp27 oligomerization, chaperone function, and protective activity against oxidative stress/tumor necrosis factor α by phosphorylation. J Biol Chem. 1999; 274:18947–56. [PubMed: 10383393]

Rogers DC, Campbell CA, Stretton JL, Mackay KB. Correlation between motor impairment and infarct volume after permanent and transient middle cerebral artery occlusion in the rat. Stroke. 1997; 28:2060–6. [PubMed: 9341719]

Rose L, Bakal DA, Fung TS, Farn P, et al. Tactile extinction and functional status after stroke. A preliminary investigation. Stroke. 1994; 25:1973–6. [PubMed: 8091440]

Saleh A, Srinivasula SM, Balkir L, et al. Negative regulation of the Apaf-1 apoptosome by Hsp-70. Nat Cell Biol. 2000; 2:476–83. [PubMed: 10934467]

Samali A, Orrenius S. Heat shock proteins: regulators of stress response and apoptosis. Cell Stress Chaperones. 1998; 3:228–36. [PubMed: 9880235]

Schallert T, Upchurch M, Lobaugh N, Farrar SB. Tactile extinction: distinguishing between sensorimotor and motor asymmetries in the rats with unilateral nigrostriatal damage. Pharmacol Biochem Behav. 1982; 16:455–62. [PubMed: 7079281]

Sharp F, Massa SM, Swanson RA. Heat shock protein protection. Trends Neurosci. 1999; 22:97–9. [PubMed: 10199631]

Thomas DL, Lythgoe MF, Pell GS, Calamante F, et al. The measurement of diffusion and perfusion in biological systems using magnetic resonance imaging. Phys Med Biol. 2000; 45:R97–138. [PubMed: 10958179]

Wegener S, Weber R, Ramos-Cabrer P, et al. Temporal profile of T2-weighted MRI distinguishes between pannecrosis and selective neuronal death after transient focal cerebral ischaemia in the rat. J Cereb Blood Flow Metab. 2006; 26:38–47. [PubMed: 15988477]

Wong EC, Cox RW, Song AW. Optimized isotropic diffusion weighting. Magn Reson Med. 1995; 34:139–43. [PubMed: 7476070]

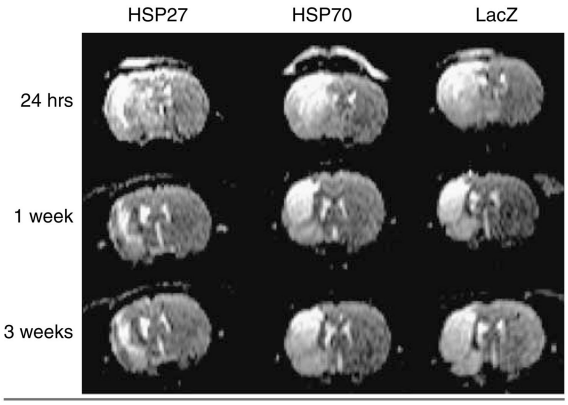

Timepoint	Lesion size (mm^3)		
	HSP27	HSP70	LacZ
24 hours	60 ± 12.4	68.6 ± 7.0	71.5 ± 7.5
72 hours	60 ± 8.5	69.9 ± 5.2	73.3 ± 4.6
1 week	59.6 ± 9.9	65.2 ± 4.1	73.3 ± 4.9
2 weeks	44.5 ± 9.2	71.4 ± 3.6	74.7 ± 6.0
3 weeks	44.8 ± 10.7	57.5 ± 4.4	69.6 ± 4.4
4 weeks	41.4 ± 10.4	64.9 ± 5.1	71.9 ± 3.8

Figure 1.
Representative centre slices (slice 5) of multislice T_2-weighted spin echo data sets. The scans show the lesion area (bright) in HSP27-, HSP70-, and LacZ-injected rats at 24 h, 1 week, and 3 weeks after MCA occlusion. Values represent absolute lesion volume (mm^3±s.e.m.) determined on multislice T_2-weighted scans per treatment group at all time points.

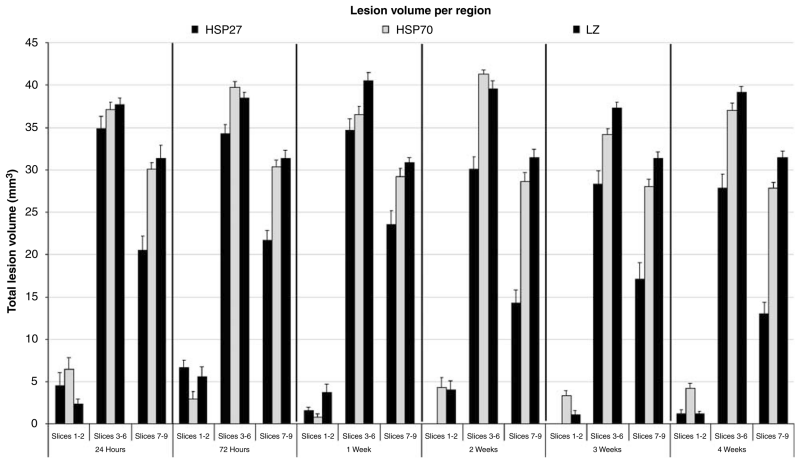

Figure 2.

Regional analysis of absolute lesion volume estimates in frontal (1 and 2), mid (3, 4, 5, and 6), and posterior (7, 8, and 9) slices calculated form multislice T_2-weighted spin echo images at six different time points in HSP-treated and control animals.

Europe PMC Funders Author Manuscripts

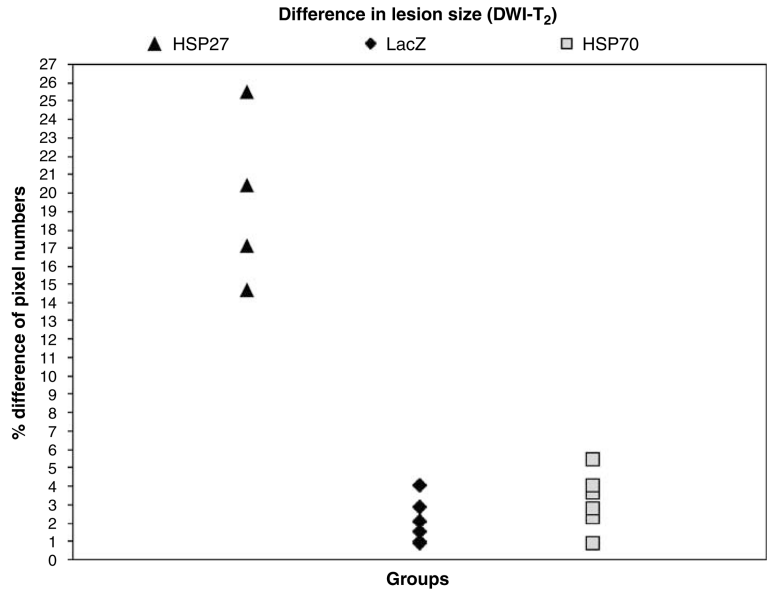

Figure 3.
Percentage difference in lesion size at 24 h after stroke calculated from single-slice DWI and T_2-weighted images. The mismatch between the lesion area calculated from ADC maps and the lesion defined on T_2-weighted images is larger in HSP27-treated animals than in HSP70-treated or control animals.

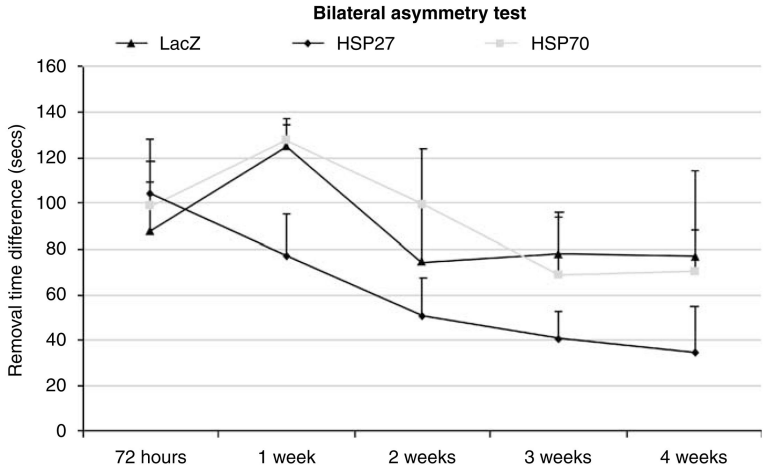

Figure 4.
Difference in the time to removal of the sticky tape from the affected paw (left) in HSP-treated and control animals up to 1 month after stroke.

Europe PMC Funders Author Manuscripts

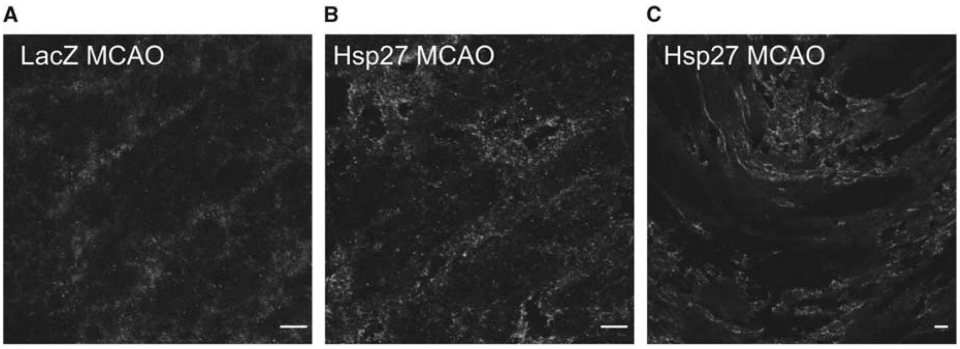

Figure 5.

Representative end-point cryosections of HSP27-injected animals and LacZ-injected controls stained for HSP27 (red) and synaptophysin (green) (63×10). (**A**) LacZ-injected and MCA-occluded control showing no colocalization of HSP27 and synaptophysin. (**B**) HSP27-injected and MCA-occluded animal stained for the same proteins showing no colocalization. (**C**) Detail of the scar edge in an HSP27-injected animal (scale bar: 10 μm).

Europe PMC Funders Author Manuscripts

Table 1

CBF measurements obtained at six time points after 30 mins of MCA occlusion in HSV-HSP27, HSV-HSP70, and control animals

CBF measurements per time point			
	% $CBF_{ipsi/contra}$		
Time point	***HSP27***	***HSP70***	***LacZ***
24 h	85.5±5	90.6±8.7	76.1±7.8
72 h	85.9±2.8	86.6±5.6	84.3±5.1
1 week	96.3±3.4	90.25±1.5	93.1±4.5
2 weeks	97.51±4.5	92.8±1.7	89.7±4.4
3 weeks	89.9±2.5	88.5±4.2	86.7±3.5
4 weeks	96.8±2.3	87±4.8	87.5±4.1

Values represent averaged CBF in the ipsilateral hemisphere as a percentage of the contralateral flow values (% $CBF_{ipsi/contra}$)±s.e.m.

Europe PMC Funders Author Manuscripts

Table 2

Total number of steps and percentage of correct steps with the affected paw (L, left) in HSV-HSP27-, HSV-HSP70-, and HSV-LacZ-injected rats at all time points

Foot-fault test						
	HSP27		*HSP70*		*LacZ*	
Time point	*Total*	*% correct L*	*Total*	*% correct L*	*Total*	*% correct L*
72 h	32.5	73.4	26.7	53.5	27.3	57.2
1 week	24.7	74.4	23.5	45.1	25.1	51.5
2 weeks	25.0	87.3	19.8	48.4	26.8	60.5
3 weeks	29.5	85.0	21.5	50.1	22.5	59.7
4 weeks	22.4	82.8	20.3	53.1	22.6	68.8

J Cereb Blood Flow Metab. Author manuscript; available in PMC 2009 June 26.